BJMS
Borneo Journal of Medical Sciences

ORIGINAL ARTICLES

Sustainable Aluminium Ion Removal Using Agro-Waste-Derived Activated Carbon for River Preservation: From Lab-Scale Towards Upscaling Study

Hui Tze Lee[1]*, Henry Chee Yew Foo[2], Yee Yong Tan[1], Inn Shi Tan[2], Shiew Wei Lau[2]

[1] Department of Civil and Construction Engineering, Curtin University Malaysia, Lot 13149, Block 5 Kuala Baram Land District, CDT 250, 98009 Miri, Sarawak, Malaysia.
[2] Department of Chemical and Energy Engineering, Curtin University Malaysia, Lot 13149, Block 5 Kuala Baram Land District, CDT 250, 98009 Miri, Sarawak, Malaysia.

*Corresponding author's email: huitze.lee@postgrad.curtin.edu.my

Received: 30 September 2025

Accepted: 15 December 2025

Published: 13 July 2026

DOI: https://doi.org/10.51200/bjms.v20iSuppl.7982

Keywords: *Sustainable aluminium removal, Agro-waste, Activated carbon, Upscaling adsorption*

ABSTRACT

High heavy metal content in river water has been a threat to the ecosystem due to bioaccumulation and biomagnification. The Miri River was deemed unsuitable for recreational use with body contact. It requires conventional treatment if used for water supply, primarily due to its high aluminium (Al) content. This is due to the anthropogenic influences of the industrial areas upstream of the river. The Al could flow into the river due to surface runoff or wastewater discharge. This study synthesised an effective adsorbent from recycled agro-waste, specifically coconut shells (CS), obtained from local areas, for Al removal. The CS was continuously produced in association with a large amount of coconut production. The current study aims to address the local water pollution issue with locally available sources to maximise environmental benefits. Under optimal conditions, the adsorbent is able to remove up to 99.84% of Al from synthetic water on a laboratory scale, reducing the concentration from 58.81 mg/L to 0.10 mg/L. A larger-scale application was examined by implementing a floating prototype with an adsorbent pack placed on it, where a residual Al content of approximately 0.06 mg/L was obtained. Moreover, the thermodynamic study validated that the Al adsorption is not limited by temperature. The efficiency remains above 99.84% with a temperature range from 25°C to 60°C . The current study demonstrates the technical feasibility of Al removal on a larger-scale

application by an adsorbent derived from recycled waste. These findings determined that the local agro-waste CS is an efficient adsorbent source for heavy metals remediation, particularly for the Miri River. A future study is required to focus on the installation of the system at other contaminated rivers.

INTRODUCTION

Heavy metal is metal with an elemental density larger than 5 g/cm3 (Ali et al., 2019). A metal element is also categorised as a heavy metal when its atomic number is greater than 20 or the atomic weight is between 63.5 and 200.6 (Ali et al., 2019; Fu & Wang, 2011). Some examples of heavy metals include Al, tin (Sn), lead (Pb) and cadmium (Cd). These heavy metals are often released to the environment, particularly rivers, due to anthropogenic factors, threatening the ecosystem when the concentration surpasses the threshold values listed in the Water Quality Standards (Department of Environment, 2025; World Health Organization, 2021). There are five primary sources of heavy metals in river due to rapid urbanisation and industrialisation, including 1) anthropogenic industrial sources such as wastewater discharge, mining and smelting, 2) agricultural sources including pesticides and fertilizers, 3) domestic waste and wastewater discharges, 4) fossil fuels combustion contributing to heavy metals release such as Cd, and 5) natural sources due to weathering of rocks (Ali et al., 2019).

Inorganic heavy metals can persist in the environment for long periods and accumulate through bioaccumulation and biomagnification. These processes increase the concentration of the heavy metals in organisms through trophic transfer (Ali et al., 2019; Blowes et al., 2014). Humans at the highest trophic level would then be exposed to the concentrated heavy metals, including Al, by consuming the contaminated food sources. Previous studies reported the health impact of excessive intake of Al, such as Alzheimer's disease, carcinogenic and genotoxic diseases (Khodapanah et al., 2013; Othmani et al., 2020). A recent case report claimed that a woman who presented with altered mental status had been diagnosed with aluminium toxicity from the measured 534 µg/L serum aluminium level. Nevertheless, this was reduced by more than 50% after nine months of daily haemodialysis (Mutugi et al., 2025). For organisms, including plants and fish, heavy metals are absorbed and accumulate in their tissues. Fish provide around 20% of the average per capita protein intake for 1.5 billion people globally (Raychaudhuri et al., 2025). This would be a significant route of Al intake by humans; hence, it is crucial to remediate Al ions from water bodies.

The Miri River in Sarawak, Malaysia, has been detected to have an excessive Al concentration (0.2 mg/L), exceeding the standard limit of 0.06 mg/L for Class IIA/IIB water as outlined in the National Water Quality Standard for Malaysia (NWQSM). Hence, the Miri River water (MRW) was classified as not suitable for recreational use with body contact and requires conventional treatment for water supply (Department of Environment, 2025). The high Al concentration could be sourced from the municipal and industrial wastewater discharge, as the riverside is occupied with industrial and residential areas. Additionally, surface runoff from workshops and construction sites along the river may contain measurable concentrations of Al, potentially degrading the water quality. Interventions are required to retrieve the Al ions from the Miri River to prevent further bioaccumulation and biomagnification.

Heavy metals remediation from the environment can be done in several ways, which are adsorption (Liang et al., 2020; Lo et al., 2012; Mkilima et al., 2024; Pandey et al., 2023), biological remediation by microbes, sometimes in conjunction with wetland and plants (Abbas et al., 2026; Shi et al., 2024), membrane filtration (Azmi et al., 2025) and precipitation (Zhao et al., 2026). Adsorption stands out from these solutions, attributed to its ease of operation and cost-effectiveness. It is often performed using activated carbon (AC) as the adsorbent. The primary concerns regarding adsorption are the precursor materials. Woods are the main source of the precursor to produce AC. However, the widespread use of AC leads to the depletion of raw materials and causes an increasing cost for both the precursor and the product. Hence, synthesising sustainable and economical adsorbents from recycled waste has become a recent trend. Al-Asadi et al., (2023) has used fig leaf AC to remediate methylene blue. Lemon peel waste was used in Pérez et al., (2023) study for copper ion removal. Meanwhile, lead and copper ions removal using the date palm fibre AC was studied by Melliti et al., (2023). These studies demonstrate the potential of biomass-derived AC in the remediation of the heavy metal Al.

Besides the material cost, the valorisation of local waste in producing AC is highly encouraged for turning the waste into a valuable material for water treatment. The yearly coconut production in Malaysia reaches 650,000 tons, with Sarawak as the state of most coconut production. This large production was associated with a large amount of coconut waste in the form of shell, trunk or fibre (Chin et al., 2021). The disposal of continuously produced coconut waste requires a large disposal area and machinery costs, which could also lead to further environmental problems. Hence, this study evaluates the feasibility of recycling local coconut waste, particularly the coconut shell, in producing AC for Al removal from water. This study aims to address local environmental threats using locally accessible raw materials to enhance sustainability. Sodium hydroxide (NaOH) was used as the activating agent due to its wide accessibility, effectiveness in pore development, and greater environmental friendliness compared to other agents, including KOH and ZnCl2. The Al removal study was conducted on synthetic water and MRW for practical application analysis, where the practical application was conducted in an upscaling setup. The effect of salinity was also studied to consider the change in water salinity during high tide or from the wastewaters. Moreover, the adsorption kinetics, isotherms, and thermodynamics were studied to gain a deeper understanding of the adsorption behaviour. Most previous studies are limited to lab-scale testing only, lacking intermediate testing of the adsorbent's performance to advance to industrial applications. It is thus included in the current study, which investigates the effectiveness of waste-derived AC in an upscaling setup, serving as an intermediate testing stage before transitioning to industrial-scale application.

MATERIALS AND METHODS

2.1 Materials and Chemicals

CS was collected from the local area in Sarawak. Aluminium chloride (AlCl3), sodium hydroxide (NaOH), and hydrochloric acid (HCl) were purchased from Sigma Aldrich (M) Sdn. Bhd. AlCl3 was used as the source of heavy metals for the preparation of synthetic water. 1 M and 0.01 M of NaOH and HCl were used to tune the water pH to the desired value. Sodium Chloride (NaCl) was used to adjust the water salinity.

2.2 Synthesis of Coconut Shells Activated Carbon

The CS collected was cleaned, washed, and oven-dried at 110^{o}C for 24 hours. A heavy-duty blender was used for grinding the CS. The ground CS was sieved with 1.18 mm and 2.36 mm sieves, where the CS that passed through the 2.36 mm sieve, while retained on the 1.18 mm sieve, was collected for further processing. The sieved CS were then carbonised with a tube furnace at a temperature of 600^{o}C for 3 hours under an inert atmosphere with argon gas. The carbonised carbon was referred to as unactivated carbon (UACCS).

Thereafter, the UACCS was impregnated in a 2.0 M NaOH solution with a ratio of 4 (150 mL NaOH : 37.5 g UACCS) for 24 hours before the activation process at 85°C for 2 hours. Next, the solution was filtered, and the residual coconut shell-activated carbon (ACCS) was oven-dried for 24 hours at 110°C. It was then washed with 1.0 M HCl and ultrapure water until a neutral pH was obtained and then oven-dried. The ACCS was ready for use when a constant weight was obtained. Figure 1 illustrates the experimental workflow diagram, from ACCS synthesis to upscaling study.

2.3 Activated Carbon Characterisation

The microstructure of the carbon materials was observed using Scanning Electron Microscopy (SEM) (Thermo Scientific Quattro S model) at an accelerating voltage of 20 kV. The thermal stability and decomposition under increasing temperature were studied with Thermogravimetric Analysis (TGA) (Mettler Toledo Thermogravimetric Analyser (TGADSCI; 1600)). Additionally, the elements and inorganic material content of the carbon materials were analysed using an Elemental Analyser (EA) with a Perkin Elmer/2400 series I model and X-ray Fluorescence (XRF) with a Bruker S2 PUMA model. The functional groups were identified using a Fourier-Transform Infrared Spectroscopy (FTIR) Cary 630 model from Agilent Technologies, with a scanning range of 650 cm-1 to 4000 cm-1 and a resolution of 4 cm-1. Total surface area and pore volume were determined by Brunauer-Emmett-Teller (BET) analysis using a Micromeritics ASAP 2020 under an inert (N2) atmosphere. The prior degassing step was performed at a temperature of 150°C for six hours with N2 gas.

2.4 Contaminated Water Samples

Synthetic Al-containing water was prepared by dissolving AlCl3 in ultrapure water to form a 1000 mg/L stock solution with a pH of 3.92. For practical study, the MRW was collected from the riverbank (4.434618, 114.001563) during high tide, ensuring the involvement of the salinity effect. The water pump was placed at a point within one meter of the bank and at a depth of one meter.

2.5 Adsorption Test

Synthetic Al-containing water was prepared and used in the optimisation study to evaluate the effectiveness of ACCS under controlled conditions. The parameters studied are pH, adsorbent dosage, initial Al concentration, and water salinity. Table 1 below shows the range of the parameters. A wide range of pH

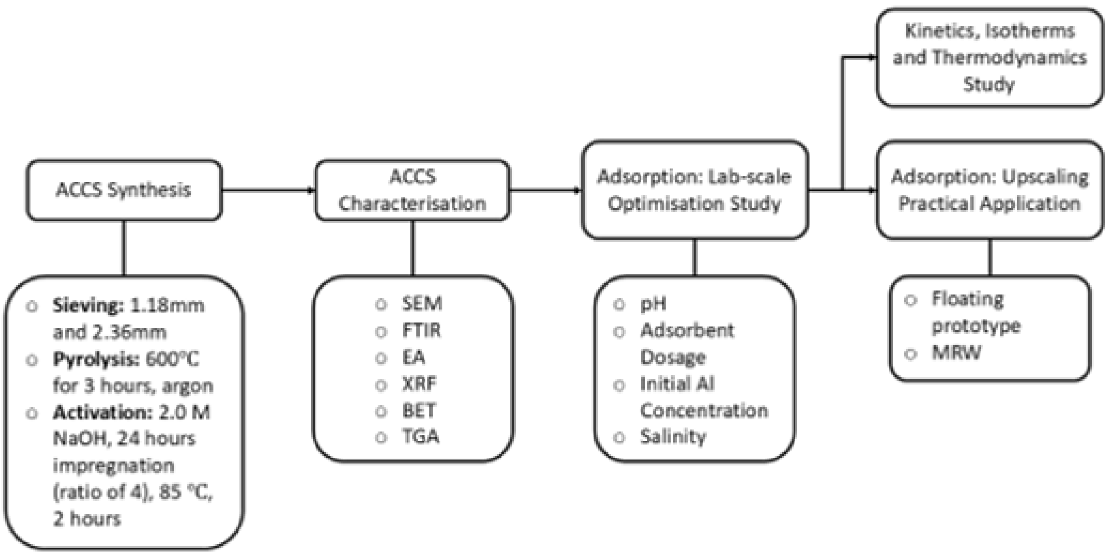

Figure 1: Experimental workflow diagram of the current study

and salinity levels was chosen in this study, considering the possible extreme water quality conditions resulting from varying severities of wastewater discharge from municipal or industrial processes. The adsorption test was conducted with a conical flask shaker at 200 rpm, and the residual Al content was measured by inductively coupled plasma optical emission spectroscopy (ICP-OES). Optimum condition was obtained using the one-factor-at-a-time approach. Previous research has reported that the typical equilibrium adsorption time for heavy metals ranges from 60 minutes to 120 minutes (Kazmierczak-razna et al., 2021; Melliti et al., 2023), with 120 minutes specifically noted for Al adsorption (El-Nahas et al., 2021). Hence, the Al adsorption optimisation study was carried out for 120 minutes or 2 hours in triplicates. The optimum conditions obtained were applied in the adsorption characteristics study for single-run experiments.

Table 1: Parameters and the ranges studied

Parameters	Ranges
pH	4 – 12
Adsorbent Dosage (g/L)	1 – 10
Initial Al Concentration (mg/L)	10 – 100
Salinity (g/L)	0 – 80

2.5.1 Adsorption Kinetics

The kinetics of the Al ion removal via ACCS have been studied under the optimum conditions. Five samples were collected periodically up to 4 hours. The adsorption capacity was calculated with (1). The data collected were fitted to pseudo-first (2) and pseudo-second (3) order kinetic models to determine the best-fit kinetic model (Amadou Kiari et al., 2024; Chan et al., 2024).

$$q_e = \frac{(C_0 - C_e) \times V}{m} \quad (1)$$

$$\log(q_e - q_t) = \log q_e - \frac{k_1}{2.303} t \quad (2)$$

$$\frac{t}{q_t} = \frac{1}{k_2 q_e^2} + \frac{1}{q_e} t \quad (3)$$

2.5.2 Adsorption Isotherm

The adsorption characteristic was further examined by studying the adsorption isotherm. The Langmuir and Freundlich models, which assume monolayer and multilayer adsorption, were applied. The experiments were conducted under the optimised conditions. Five samples with initial Al concentrations of 10 mg/L, 32.5 mg/L, 55 mg/L, 77.5 mg/L, and 100 mg/L were prepared. Samples were collected and tested once the equilibrium had been reached. The concentration of Al in the solution at equilibrium, Ce (mg/L), and the amount of Al ion adsorbed per unit mass of AC at equilibrium, qe (mg/g), were determined. The linear expressions of the Langmuir (4) and Freundlich (5) models are shown below (Amadou Kiari et al., 2024). The best-fit model was determined by the highest R2 coefficient.

$$\frac{1}{q_e} = \frac{1}{q_m} + \frac{1}{K_L q_m} \times \frac{1}{C_e} \quad (4)$$

$$\log q_e = \log K_F + \frac{1}{n} \log C_e \quad (5)$$

2.5.3 Adsorption Thermodynamics

The Al removal efficiency of the ACCS at different temperatures was analysed. Temperatures of 25°C, 30°C, 40°C, 50°C, and 60°C were tested under optimum conditions. Parameters including Gibbs free energy, ΔG°, enthalpy change, ΔH°, and entropy change, ΔS°, were calculated by applying equations (6), (7), and (8), respectively (Amadou Kiari et al., 2024). By studying the adsorption thermodynamics, the effect of temperature on the Al removal process can be identified.

$$\Delta G° = -RT\ln K \quad (6)$$

$$\Delta G° = \Delta H° - T\Delta S° \quad (7)$$

$$\ln K = -\frac{\Delta H°}{RT} + \frac{\Delta S°}{R} \quad (8)$$

2.5.4 Upscaling Adsorption Test

The upscaling Al removal process was conducted using an innovative setup of a commercial floating structure prototype. The prototype has dimensions of 330 mm x 305 mm x 254 mm and a flow rate of 2.2 m3/hr. The operating concept mainly relies on the built-in pump that pumps the surrounding water to flow through the prototype from top to bottom, thereby filtering the debris and Al ions. As water passes through the system, the Al ions are adsorbed by the ACCS. The prototype was loaded with 100 g of ACCS. Figure 2 below shows the schematic diagram of the prototype. Then, it was placed in a container filled with raw MRW without any modifications. The upscaling study aims to evaluate the feasibility of ACCS in larger-scale applications for Al removal, which is a preliminary study and a crucial step towards field application at the Miri River. The practical application of the ACCS was analysed by determining the Al content in the river water after 24 hours.

RESULTS AND DISCUSSIONS

3.1 Level of Contamination in Miri River

The MRW collected has undergone ICP-OES to determine the heavy metal content, and compared to the Class IIA/IIB water quality requirement in the NWQSM (Department of Environment, 2025). The results are tabulated in Table 2. Water sources categorised under Class IIA are used in water supply and fishery, whereas water under Class IIB is for recreational use with body contact. The results show that calcium (Ca), magnesium (Mg), and Al ions in the Miri River have exceeded the standard limits noted in NWQSM. The excess Al content would be sourced from surrounding factories or construction sites, where Al ions flow into the Miri River through surface runoff or wastewater discharge. Besides, the high Ca and Mg content can be attributed to both natural and anthropogenic factors, including carbonate weathering and runoff or effluent discharge from nearby industries. The higher Mg content could be attributed to the production and use of alloys by industrial sectors. Meanwhile, it was reported that carbonate weathering has dominated Mg isotopes in the riverine system, including the Yangtze River, Jinsha Jiang, Lancang Jiang, and Nu Jiang (Y. Xu et al., 2022, 2023).

The current study focused solely on Al ions, as Ca and Mg ions are essential for organisms. It was reported that the use of calcium as one of the supplements has increased the yield and quality of Mentha spicata essential oil by enhancing photosynthesis, increasing chlorophyll content and the antioxidant and antibacterial activity (L. Xu et al., 2024). Additionally, utilising calcium-rich feed for young heifers was claimed to enhance the digestibility of nutrients such as cellulose,

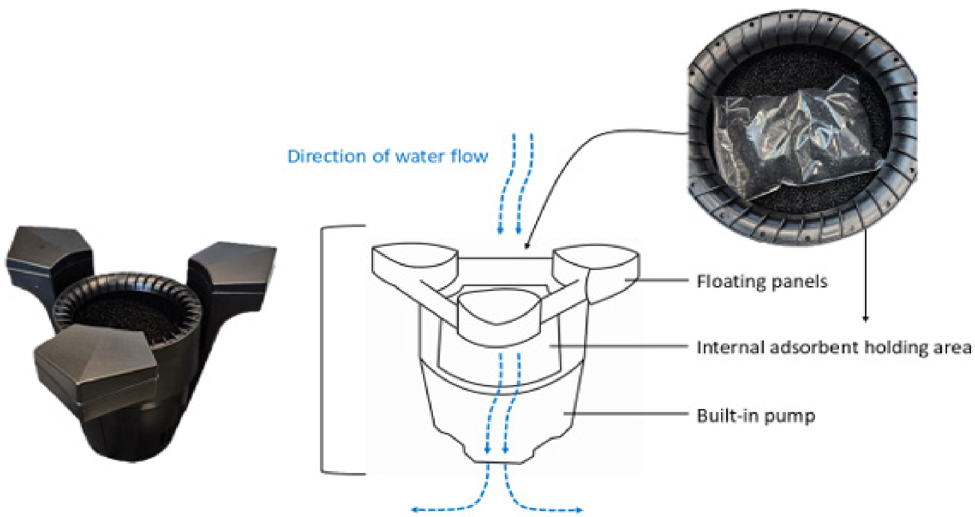

Figure 2: Schematic diagram of the floating prototype showing the parts of the prototype and the direction of water flow

hemicellulose and crude protein (Bhagat et al., 2025). Similarly, Mg enhances plant growth by increasing chlorophyll content, promoting nutrient uptake, and improving seed germination (Chitrashalini & Kumar, 2025). For animals and humans, Mg deficiency results in depressed immune responses. Mg plays a significant role in activating vitamin D, the lack of which may contribute to cytokine storm and result in infectious diseases such as COVID-19 (Dinicolantonio & O'keefe, 2021; Dominguez et al., 2021).

3.2 Activated Carbon Characterisation

3.2.1 Adsorbent Microstructure

The density of the ACCS was measured to be 1 g/cm^3. For the microstructure, SEM was used to observe the morphological properties of the materials. Figure 3 shows the microstructure of the carbon materials, which was captured at 5000x magnification. The SEM image shows that the ACCS was more porous compared to the UACCS, reflecting the improved adsorption efficiency. This is a result of the penetration of the activating agent into the carbon materials, forming a more porous structure.

3.2.2 Surface Functional Groups

Figure 4 shows the FTIR spectra of the carbon materials. Stronger peaks are observed for the ACCS, indicating the increased effectiveness after activation. The wide peak within wavenumbers 3200 cm-1 and 3700 cm-1 corresponds to the O-H stretching vibrations associated with hydroxyl groups (Bampi et al., 2024; Chan et al., 2024). The denser peak by the ACCS suggests a higher concentration of hydroxyl groups, which were introduced during the activation process. Next, the sharp peak located at 1600 cm-1 corresponds to the C=O stretching vibrations from carbonyl groups. More oxygenated groups in the ACCS were validated by the slightly denser peak (Amadou Kiari et al., 2024). Another sharp peak between 1000 cm-1 and 1200 cm-1 corresponds to C-O stretching vibrations, in which a stronger peak is also observed for the ACCS (Gao et al., 2024). The increased number of oxygen-containing functional groups measured for ACCS verifies the successful activation of the pyrolysed coconut carbon by NaOH.

3.2.3 Chemical Composition

The elemental composition of CS, UACCS, and ACCS was analysed and shown in Table 3. It was observed that the carbon content of CS before and after carbonisation is similar. Meanwhile, the carbon content has increased by approximately 96% after activation, with other elements present in trace amounts, suggesting that the activation process has enhanced both the carbon purity and the adsorption capacity.

Table 2: Heavy metals content in Miri River

Heavy Metal Ions	Results	Class IIA/IIB	Unit
Copper	ND <0.01	0.02	mg/L
Calcium	65.30	250.00	mg/L
Magnesium	302.30		mg/L
Iron	0.80	1.00	mg/L
Manganese	0.04	0.10	mg/L
Sulphide	ND <0.10	-	mg/L
Aluminium	0.20	0.06	mg/L
Zinc	ND <0.02	5.00	mg/L
Lithium	ND <0.10	-	mg/L

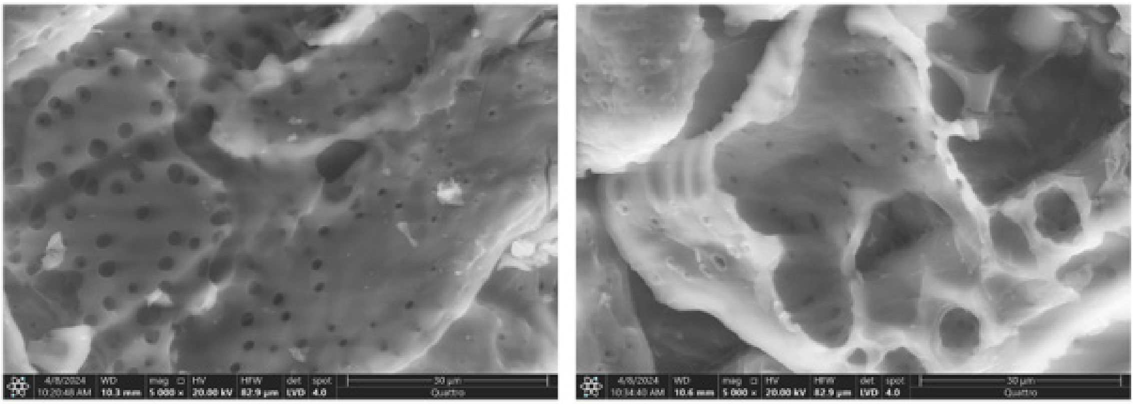

(a) (b)

Figure 3: SEM images of (a) UACCS and (b) ACCS

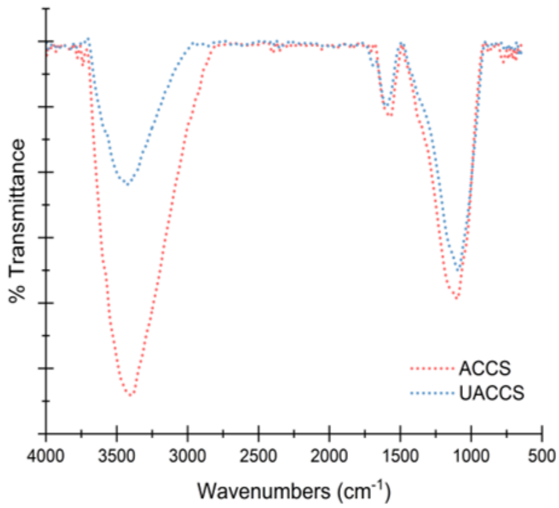

Figure 4: FTIR spectrum for UACCS and ACCS

3.2.3 Chemical Composition

The elemental composition of CS, UACCS, and ACCS was analysed and shown in Table 3. It was observed that the carbon content of CS before and after carbonisation is similar. Meanwhile, the carbon content has increased by approximately 96% after activation, with other elements present in trace amounts, suggesting that the activation process has enhanced both the carbon purity and the adsorption capacity.

Table 3: Elemental composition of the raw material (CS) and the carbon materials

Sample Name	CS	UACCS	ACCS
Carbon (%)	48.21	44.20	86.62
Hydrogen (%)	5.38	1.83	3.24
Nitrogen (%)	0.20	0.32	0.40
Sulphur (%)	0.46	0.22	0.15
Others (%)	45.75	53.43	9.59

Besides elemental content, the inorganic composition in ACCS was determined by XRF and tabulated in Table 4. The inorganic content analysed would be the 9.59% of undetected residual content in the EA results. It was determined that the predominant inorganic content is Mg (51.02%), followed by silica (16.48%) and potassium (12.98%), with other negligible elements. While potassium oxide (35.13%), calcium oxide (19.22%), and iron (III) oxide (10.14%) are the basic inorganic metal oxides determined on ACCS. The presence of these materials is attributed to the composition of the precursor, CS, that persists after the carbonisation and activation process (Moujoud et al., 2023; Ranatunga et al., 2023).

3.2.4 Pore Size and Total Surface Area

A smaller pore size allows the adsorption of smaller-sized adsorbates, while a higher surface area ensures better adsorption capacity. The specific surface areas of the coconut materials were determined by BET analysis and are shown in Table 5. Non-measurable pore size was detected for CS, indicating a smooth, solid surface with nearly no pores. This was verified by the low surface area of 1.02 m2/g. The

Table 4: XRF results of ACCS

Element	Concentration (%)	Metal Oxide	Concentration (%)
Mg	51.02	MgO	3.97
Al	8.36	Al2O3	0.00
Si	16.48	SiO2	0.00
P	0.95	P2O5	4.57
S	1.01	SO3	6.26
Cl	2.49	Cl	4.61
K	12.98	K2O	35.13
Ca	3.94	CaO	19.22
Ti	0.47	TiO2	3.40
Cr	0.10	Cr2O3	1.48
Mn	0.11	MnO	1.48
Fe	1.66	Fe2O3	10.14
Zn	0.43	ZnO	2.27

surface area was observed to be effectively enhanced by approximately 4000% after the pyrolysis process, with a value of 41.85 m^2/g determined for UACCS. However, this has been reduced after the activation process, with an increment in pore size noted. The pore size was increased from 2.05 nm to 2.98 nm after activation. The phenomenon could be attributed to the relatively low-energy or low-temperature activation process, which only fosters the penetration of UACCS by NaOH on the surface, thereby developing pores in the lateral direction, but not in depth to the carbon core. Compared to the coconut AC composites in a study by Li & Zhu, (2024), the pore size measured was greater than the 2.07 nm from the study. However, the surface area measured in the current study is slightly lower than the 22.7 m2/g reported in Li & Zhu, (2024) study.

Figure 5 shows the curves obtained from the BET analysis. The N2 adsorption-desorption isotherm curve in Figure 5(a) denotes an IUPAC Type IV isotherm profile with a H3 hysteresis loop (Muttakin et al., 2018). The unclose isotherm curves under P/P0<0.45 imply the presence of a swelling phenomenon in the sample. The isotherm profile characterises the slit-shaped mesopores as the main pore morphology of ACCS (Rouquerol et al., 1994; Song et al., 2023). Meanwhile, the BJH desorption pore size distribution (dV/dlog(w)) in Figure 5(b) shows only two bins around and greater than 500 Å or 50 nm, showing the negligible mesoporosity between 2 nm and 50 nm. This indicates that the pore distribution has been limited by the sensitivity of the BJH model, which typically suits the range from 2 nm to 50 nm. In other words, the ACCS synthesised is a larger mesoporous carbon. The BJH adsorption cumulative pore volume plot presented in Figure 5(c) further justifies the relatively large mesopore properties of ACCS. It is noted that the pore volume reduced significantly at a small pore width (10 Å to 20 Å). This was followed by a smoother decline up to 1000 Å. Overall, the mesopore volume detected was about 0.01 cm3/g, which is considerably low. Further observation from the t-plot shown in Figure 5(d) yields a y-intercept for micropore volume of 0.282 cm3/g, indicating low micropores. Hence, the curves convey that the ACCS is a meso-macroporous AC, where large mesopores dominate. The BET analysis results are supported by the SEM observation of ACCS, which shows a more porous structure with a larger pore width. However, a more specific BET analysis on macropore would be required for further validation of the justifications.

Table 5: BET surface areas of the precursor and carbon material

Sample	BET Surface Area (m2/g)	Pore Size (nm)
CS	1.02	-
UACCS	41.85	2.05
ACCS	14.66	2.98

3.2.5 Thermogravimetric Analysis

Figure 6 shows the TGA analysis results. The initial weight loss below 150°C corresponds to the evaporation of moisture. A small weight loss was observed for all samples due to their naturally low moisture content. The following decomposition stage up to 600°C is attributed to the decomposition of the oxygen-containing functional groups, such as carbonyl

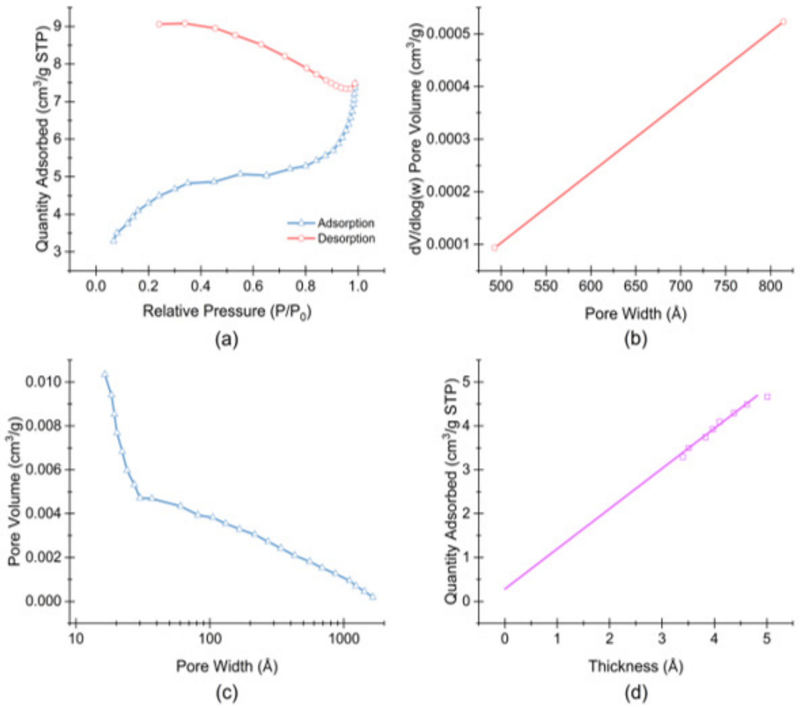

Figure 5: BET analysis results of ACCS: (a) N2 adsorption-desorption isotherm, (b) Pore size distribution - BJH desorption dV/dlog(w), (c) Cumulative pore volume - BJH adsorption and (d) t-plot

and hydroxyl groups. The greater weight loss achieved by ACCS validates the larger number of functional groups it possesses. Compared to CS, carbon materials exhibit greater thermal stability due to their lower organic content. Lastly, the weight loss after 600°C represents the breakdown of the carbon skeleton, where the gradually reduced sample weight shows the thermal stability properties of the carbon materials. The higher weight loss observed on ACCS is attributed to the greater exposure of the internal pore structure to the thermal environment compared to UACCS.

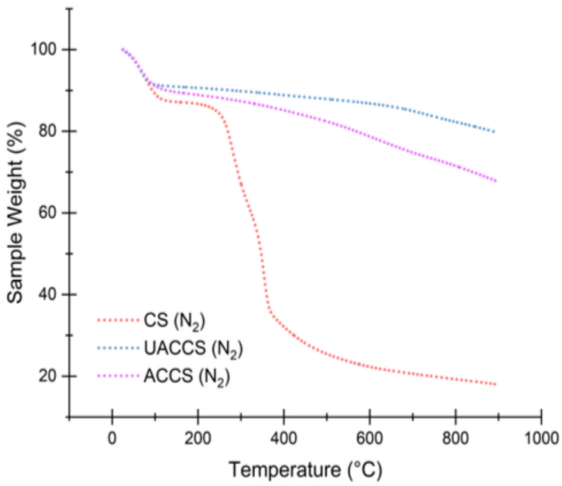

Figure 6: TGA results of the coconut shell and carbon materials

3.3 Adsorption Test

3.3.1 Optimisation Study with Synthetic Water

The optimisation study was carried out on a lab-scale with synthetic water in triplicate. When studying the effect of each parameter, the other parameters were held constant at the midpoint of their respective ranges. Figure 7 shows the resulting trend of each factor with the optimal values.

According to Figure 7(a), the Al removal efficiency increased from 61.91±1.36% to 84.20±2.92% as the solution pH increased from 2 to 8. After that, the efficiency reduced significantly to 31.00±7.55% when the pH increased to 14. This finding validated that the Al removal is more favourable under acidic conditions. In the meantime, the optimum pH for Al adsorption by ACCS was determined as 6.95. The nearly neutral optimum pH denotes that the treatment process does not require an extreme pH condition. This is much preferred for real-life applications that have constraints on the influences on the aquatic ecosystem.

Figure 7(b) presents the optimisation trend of the initial Al concentration parameter. The Al removal was maintained above 77.5% for the range tested (1 mg/L to 100 mg/L). The Al removal efficiency increased gradually, reaching 89.71±2.59% at an initial Al concentration of 55 mg/L. This was slightly reduced to 82.36±4.96% at 100 mg/L. The reduction in Al removal with increasing Al concentration indicates that the adsorption sites on the ACCS were saturated, resulting in excessive free Al remaining in the system. The optimum initial Al concentration was calculated as 58.81 mg/L.

It was observed from Figure 7(c) that Al adsorption was efficient at 85.78±5.05%, even with a low adsorbent dosage of 0.5 g/L, demonstrating the effectiveness of the ACCS. Thereafter, the Al removal increased with increasing adsorbent dosage, attributed to the availability of more adsorption sites (Tangsathitkulchai et al., 2012). The highest Al removal efficiency measured was 94.73±5.27%, associated with an adsorbent dosage of 10 g/L. This then approached a constant value when the adsorbent dosage increased further to 14.5 g/L. The optimisation study showed that an adsorbent dosage of 10.48 g/L maximised Al adsorption, indicating an optimal dosage.

The resulting trend in Figure 7(d) shows that a saline environment is not favourable for Al removal, as the removal efficiency decreases by about 5% with the addition of 20 g/L salinity. This phenomenon persisted up to a salinity of 80 g/L, with the lowest Al removal efficiency measured at 85.00±0.27%. Although Al removal was observed to decrease with more extreme saline conditions, the efficiencies remained above 85%. Nonetheless, 0 g/L salinity was determined as the optimum salinity due to the highest removal efficiency measured (94.55±0.18%).

The optimisation study shows that the greatest Al removal can be achieved with a

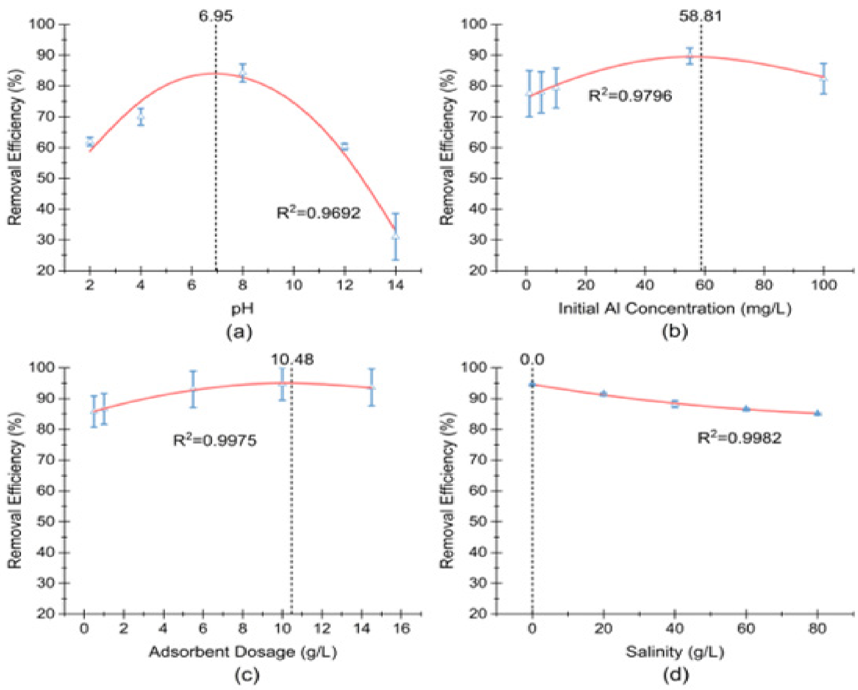

Figure 7: Optimum Al removal conditions: (a) pH, (b) initial Al concentration, (c) adsorbent dosage and (d) salinity

water pH of 6.95, an initial Al concentration of 58.81 mg/L, 10.48 g/L adsorbent dosage and 0 g/L salinity. The optimum conditions were then applied in the adsorption characteristics study, including kinetics, isotherms, and thermodynamics. Upon performing validation tests with these conditions, an Al removal of 99.84±0.01% was obtained. This is comparable to Ren et al., (2023) study of 95% Al removal using waste polyethylene terephthalate AC, and the approximately 80% Al removal by eucalyptus AC from (Tangsathitkulchai et al., 2012) study. Moreover, the granular ACCS developed in the present study exhibits a similar Al removal efficiency to a Fe-modified granular AC, which shows 95.16% Al removal (Mahdavi et al., 2018).

This finding shows the efficiency and potential of the local biomass waste as a bio-adsorbent source in treating heavy metal-polluted river water. The valorisation of the agro-waste, CS, serves as a sustainable waste management approach and produces a value-added product for river remediation.

3.3.1.1 Adsorption Kinetics

The experimental data of the kinetics study are shown in Figure 8. The results suggested that the Al adsorption is best fitted to the pseudo-second-order kinetic model. The Al adsorbed increases with time for the first 30 minutes. This is due to the availability of a large number of active sites on the adsorbent surface at the initial stage of the adsorption process (Al-Asadi et al., 2023; Amadou Kiari et al., 2024). Thereafter, the adsorbing rate has decreased and reached equilibrium at 60 minutes, corresponding to the occupation of most adsorption sites (Amadou Kiari et al., 2024). The Al ions adsorbed by the ACCS at equilibrium were determined as 5.23 mg/g. After equilibrium had been reached, the active sites on the ACCS surface were saturated, resulting in a slow adsorption process and a constant adsorption capacity. The kinetic parameters and coefficients are tabulated in Table 6.

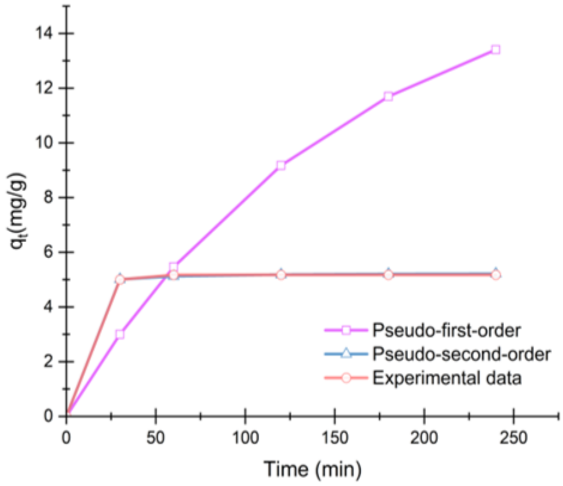

Figure 8: Comparison of experimental data to the calculated data from pseudo-first and second-order kinetic models

Table 6: Parameters of pseudo-first and second-order kinetic models

Pseudo-First-Order			
R^2	k_1 (1/min)	$q_{e,experimental}$ (mg/g)	$q_{e,calculated}$ (mg/g)
0.1942	0.0064	5.23	17.03
Pseudo-Second-Order			
R^2	k_2 (g/mg.min)	$q_{e,experimental}$ (mg/g)	$q_{e,calculated}$ (mg/g)
0.9999	0.1362	5.23	5.24

3.3.1.2 Adsorption Isotherm

The adsorption of Al ions onto the ACCS was best described by the Langmuir isotherm model (R^2 = 0.9978), followed by the Freundlich model (R^2 = 0.9804). The parameters were tabulated in Table 7. This suggests that the monolayer adsorption mechanism dominated the Al adsorption process. The finding is similar to that from Chan et al., (2024) study on the adsorption of methylene blue by the coconut shell-derived AC. The results suggest that the adsorption process is taking place with a fixed number of adsorption sites. There is no lateral interaction or transmigration of the Al ions in the plane of ACCS, in which all the adsorbate molecules are experiencing equal enthalpies and activation energies (Waheed et al., 2021).

Table 7: Adsorption isotherm parameters for Langmuir and Freundlich models

Langmuir			Freundlich		
R^2	q_m	k_L	R^2	n	k_F
0.9978	94.3396	0.0083	0.9804	1.0458	0.7943

3.3.1.3 Adsorption Thermodynamics

Al removal process under 25°C, 30°C, 40°C, 50°C, and 60°C was investigated. Thermodynamic parameters including ΔG°, ΔH° and ΔS° were obtained from the linear regression of lnK against 1/T (Figure 9), where temperature is in Kelvin. Table 8 presents the thermodynamic parameters. The ΔG° values obtained were all negative, indicating the spontaneous nature of the adsorption process. Meanwhile, a ΔG° value greater than -20 kJ/mol suggests physisorption, whereas a value smaller than -40 kJ/mol corresponds to chemisorption, and those between -20 kJ/mol and -40 kJ/mol denote a mixed physisorption/ chemisorption (Amadou Kiari et al., 2024; Kokalj, 2022, 2026). Hence, the ΔG° values obtained, which range between -17.66 kJ/mol and -15.80 kJ/mol, indicate that physisorption as the predominant adsorption mechanism involved in the Al adsorption process. Besides, the negative ΔH° value (-0.1720 kJ/mol) indicates that the adsorption process is slightly exothermic. Associated with the consistent Al removal efficiency obtained across all the temperatures tested, it was suggested that the Al adsorption process by ACCS is thermally insensitive. The Al removal process is potentially dominated by physisorption or weak surface-driven adsorption. This occurred through the surface affinity and diffusion of Al ions into the pores of ACCS, rather than through heat-driven chemical bonding. As a result of the optimisation study, where an optimum pH of 6.95 was determined, the O-H, C=O and C-O functional groups identified from FTIR analysis would not deprotonate at this near-neutral pH. Hence, the possibility of Al adsorption by electrostatic attraction to the functional groups and chemically bonding is lower than that of adsorption and trapping by the pores on ACCS. This was supported by the near-zero enthalpy, ΔH° obtained. Lastly, the positive ΔS° value indicates the increase in randomness and degree of freedom of the adsorption process (Amadou Kiari et al., 2024; Sahmoune, 2019). The thermodynamics results show that the adsorption process is dominated by physisorption, with a weak contribution from a heat-driven chemical bonding process (Amadou Kiari et al., 2024; Garikoé et al., 2020). This has resulted in an average Al removal of 99.84% at all temperatures, with minimal impact on the water quality in terms of temperature.

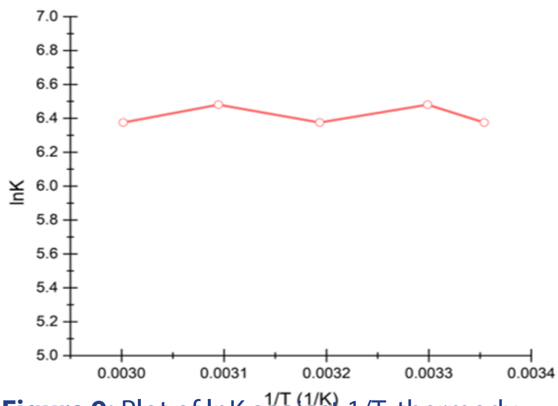

Figure 9: Plot of lnK against 1/T, thermodynamic studies of the Al adsorption processs

3.3.2 Upscaling Study with Miri River Water

The effectiveness of the ACCS has been evaluated with synthetic water. Its practical performance was then determined with raw MRW, which was conducted as an upscaling study with a floating prototype. A non-detectable residual Al content was obtained, indicating a value of less than 0.1 mg/L. The exact value cannot be obtained due to the limitations of the equipment. It may be essential to consider the use of higher-sensitivity equipment for detecting the residual Al content. However, the detected value of <0.1 mg/L is relatively close to the standard threshold value of Class IIA/IIB in the NWQSM (0.06 mg/L), indicating the effectiveness of ACCS in remediating the contaminant to a safe level for water supply, fisheries, and recreational activities with body contact (Department of Environment, 2025). The great Al removal efficiency with raw MRW could be partly aided by the organic matter in the river water, which traps and adsorbs the Al ions with the ACCS (Amadou Kiari et al., 2024). A beneficial effect of organic matter was also reported from (Phal et al., 2025) study, which proposed the binding of non-coagulable organic matter with AC to form new adsorptive sites. These organic matters then work in conjunction with the initial adsorption effect from ACCS in Al adsorption, thereby enhancing the Al removal efficiency.

The results suggest that the sustainable adsorbent derived from local agro-waste is efficient for lab-scale and upscaling Al adsorption and has potential in treating river water contaminated with excessive Al ions. The lab-scale kinetics study revealed that the time required to reach equilibrium was 60 minutes. A kinetic study considering the upscaling application would be necessary to determine the optimal timing for replacing the adsorbent. An imaging technique such as SEM could be a useful tool for assisting visualisation. Future studies should focus on the on-site application of the system, since the current upscaling study was conducted with a fixed volume of MRW only. Furthermore, studies on the competing effects from other heavy metals in MRW are required to gain deeper insights into the field application of the adsorbent. Regarding potential scalability challenges, the regeneration ability of the adsorbent must be assessed to further evaluate and elevate the sustainability of the adsorption process. The spent adsorbent can then be another potential resource for recovering the metals adsorbed via acid soaking or incineration.

CONCLUSION

The effectiveness of a sustainable adsorbent developed with agro-waste, CS on Al removal from synthetic water and raw MRW was investigated. Carbon materials produced by CS exhibited improved properties after activation, as evidenced by increased porosity and the presence of oxygen-containing functional groups, as observed in the SEM and FTIR results. Additionally, the carbon content has increased due to the removal of impurities and the subsequent increase in AC purity after activation.

The optimisation study suggests that the salinity was not favourable for Al adsorption, although around 85% Al removal could still be achieved under an extreme saline environment. It was determined that the optimal Al removal can be achieved with a water pH of 6.95, an initial Al concentration of 58.81 mg/L, 10.48 g/L adsorbent dosage, and 0 g/L salinity. The validation tests then showed an Al removal of 99.84±0.01%. It was determined that the pseudo-second-order and Langmuir isotherm models best describe the adsorption process, where equilibrium was reached at 60 minutes, indicating monolayer adsorption. In addition, thermodynamic studies suggest that physisorption is the predominant adsorption mechanism, characterised by an increase in randomness and degree of freedom. The Al adsorption by ACCS has been determined to be thermally insensitive with slight exothermic

Table 8: Thermodynamic parameters for the Al adsorption process

Temperature (°C)	Temperature (K)	K	ΔG° (kJ/mol)	ΔH° (kJ/mol)	ΔS° (J/K.mol)
25	298.15	587.10	-15.80	-0.1720	52.81
30	303.15	652.44	-16.33		
40	313.15	587.10	-16.60		
50	323.15	652.44	-17.41		
60	333.15	587.10	-17.66		

behaviour. This can be attributed to the near-neutral optimum pH that to a large extent did not foster the deprotonation of the functional groups. Nevertheless, an average removal efficiency of 99.84% has been achieved at all temperatures.

Raw MRW was used for an upscaling and practical application study. The residual Al content that is relatively close to the standard value of Class IIA/IIB from the NWQSM (0.06 mg/L) shows the effectiveness of the ACCS. The treated MRW was determined to be safe for the water supply, fishery, and recreational activities with body contact. Nonetheless, further studies are essential using more sensitive heavy metal detection equipment to obtain an accurate value for the residual Al content, as well as to assess the system's adaptability in varying sites. Future research on on-site studies could also consider monitoring other contaminants to further evaluate the feasibility of the adsorbent and the prototype for upscaling contaminant removal. Interactions between different parameters can be considered as future scope using Response Surface Methodology, as this was ignored in the one-factor-at-a-time approach. Meanwhile, for future on-site installations, it is recommended to install an anchor and a global positioning system (GPS) to secure and locate the system. Modification would be essential for the power supply of the pump in the prototype for long-term application. A solar power supply could be an effective alternative to overcome the limitations of the conventional power supply system. A techno-economic assessment is required to consider the economic benefits before advancing to industrial application. The success of the practical study demonstrates the ability of a local CS waste-derived adsorbent to remediate heavy metals, such as Al, from river water, thereby maintaining a safe environment for the aquatic ecosystem and contributing to reducing the effects of bioaccumulation and biomagnification.

CONFLICT OF INTEREST

The authors declare that they have no known competing financial interests or personal relationships that could have appeared to influence the work reported in this paper

ACKNOWLEDGEMENTS

The authors gratefully acknowledge the financial support provided by Curtin University Malaysia through the Curtin Malaysia Research Fund (CMRF/001145). Appreciation is also extended to the Kurita Water and Environment Foundation (KWEF/23Pmy008) for their support. In addition, the authors wish to thank Curtin University Malaysia for further support through the Curtin Malaysia Higher Degree Research (CMHDR) Grant and the Curtin Malaysia Postgraduate Research Scholarship (CMPRS).

REFERENCES

Abbas, A., Ahmad, M., Yousaf, M., Pan, L., & Xu, D. (2026). Synergistic role of microbes and wetland plants in an advanced-acclimatized constructed wetland for enhanced removal of heavy metals. Gondwana Research, 150, 274–286. https://doi.org/10.1016/j.gr.2025.09.020

Al-Asadi, S. T., Al-Qaim, F. F., Al-Saedi, H. F. S., Deyab, I. F., Kamyab, H., & Chelliapan, S. (2023). Adsorption of methylene blue dye from aqueous solution using low-cost adsorbent: kinetic, isotherm adsorption, and thermodynamic studies. Environmental Monitoring and Assessment, 195(6). https://doi.org/10.1007/s10661-023-11334-2

Ali, H., Khan, E., & Ilahi, I. (2019). Environmental chemistry and ecotoxicology of hazardous heavy metals: Environmental persistence, toxicity, and bioaccumulation. In Journal of Chemistry (Vol. 2019). Hindawi Limited. https://doi.org/10.1155/2019/6730305

Amadou Kiari, M. N., Konan, A. T. S., Sanda Mamane, O., Ouattara, L. Y., Ibrahim Grema, M. H., Siragi Dounounou Boukari, M., Adamou Ibro, A., Malam Alma, M. M., & Yao, K. B. (2024). Adsorption kinetics, thermodynamics, modeling and optimisation of bisphenol A on activated carbon based onHyphaene Thebaica shells. Case Studies in Chemical and Environmental Engineering, 10. https://

doi.org/10.1016/j.cscee.2024.100903

Azmi, L. S., Jabit, N. 'Ain, Ismail, S., Ku Ishak, K. E. H., & Abdullah, T. K. (2025). Membrane filtration technologies for sustainable industrial wastewater treatment: a review of heavy metal removal. In Desalination and Water Treatment (Vol. 323). Elsevier B.V. https://doi.org/10.1016/j.dwt.2025.101321

Bampi, J., da Silva, T. C., da Luz, C., Pasquali, G. D. L., Dervanoski, A., & Tochetto, G. (2024). Study of the competitive effect on the adsorption of phenol and 4-nitrophenol in a batch reactor and fixed-bed column using coconut shell activated carbon. Journal of Water Process Engineering, 65. https://doi.org/10.1016/j.jwpe.2024.105825

Bhagat, J., Dutta, T. K., Chatterjee, A., Mohammad, A., & Agrawal, V. (2025). Valorized by-product of marine-derived Turbinella pyrum shell-based industries: A viable source of calcium and essential trace elements for young crossbred heifers. Regional Studies in Marine Science, 91. https://doi.org/10.1016/j.rsma.2025.104553

Blowes, D. W., Ptacek, C. J., Jambor, J. L., Weisener, C. G., Paktunc, D., Gould, W. D., & Johnson, D. B. (2014). 11.5 - The Geochemistry of Acid Mine Drainage. In H. D. Holland & K. K. Turekian (Eds.), Treatise on Geochemistry (Second Edition) (2nd ed., Vol. 11, pp. 131–190). Elsevier Inc. https://doi.org/https://doi.org/10.1016/B978-0-08-095975-7.00905-0

Chan, A. A., Abdul Raman, A. A., Chong, W. L., & Buthiyappan, A. (2024). Graphene oxide impregnated activated carbon derived from coconut shell through hydrothermal carbonization for cationic dye removal: Adsorptive performance, kinetics, and chemistry of interaction. Journal of Cleaner Production, 437. https://doi.org/10.1016/j.jclepro.2024.140655

Chin, M. Y., Rahman, Md. R., Kuok, K. K., Chiew, W. Y., & Bakri, M. K. (2021). Characterization and Impact of Curing Duration on the Compressive Strength of Coconut Shell Coarse Aggregate in Concrete. Bio Resources, 16(3), 6057–6073. https://doi.org/10.15376/biores.16.3.6057-6073

Chitrashalini, S., & Kumar, S. V. (2025). Harnessing the potential of plant-mediated magnesium oxide nanoparticles: a sustainable approach towards crop management and soil health. Pedosphere. https://doi.org/10.1016/j.pedsph.2025.11.013

Department of Environment. (2025). STANDARD KUALITI AIR KEBANGSAAN & INDEKS KUALITI AIR. https://www.doe.gov.my/en/national-water-quality-standards/

Dinicolantonio, J. J., & O'keefe, J. H. (2021). Magnesium and Vitamin D Deficiency as a Potential Cause of Immune Dysfunction, Cytokine Storm and Disseminated Intravascular Coagulation in COVID-19 Patients. Missouri Medicine, 118(1), 68–73. https://pmc.ncbi.nlm.nih.gov/articles/PMC7861592/

Dominguez, L. J., Veronese, N., Guerrero-Romero, F., & Barbagallo, M. (2021). Magnesium in Infectious Diseases in Older People. Nutrients, 13(180). https://doi.org/10.3390/nu13010180

El-Nahas, S., Salman, H. M., & Saber, A. M. (2021). Production of low-price carbon for removal of aluminium ions in potable water. Journal of Environmental Engineering and Science, 16(3), 145–164. https://doi.org/10.1680/jenes.20.00055

Fu, F., & Wang, Q. (2011). Removal of heavy metal ions from wastewaters: A review. In Journal of Environmental Management (Vol. 92, Issue 3, pp. 407–418). https://doi.org/10.1016/j.jenvman.2010.11.011

Gao, Q., Ni, L., Rong, S., Liu, S., Zhong, Y., & Liu, Z. (2024). Enhancement effect of potassium ferrate on self-activation: Significant improvement in pore structure and adsorption performance of activated carbon. Bioresource Technology, 413. https://doi.org/10.1016/j.biortech.2024.131546

Garikoé, I., Sorgho, B., Yaméogo, A., Guel, B., & Andala, D. (2020). Removal of bisphenol A by adsorption on organically modified clays from Burkina Faso. Bioremediation Journal, 25(1), 22–47. https://doi.org/10.1080/10889868.2020.1842321

Kazmierczak-razna, J., Zioła-frankowska, A., Nowicki, P., Frankowski, M., Wolski, R., & Pietrzak, R. (2021). Removal of heavy metal ions from one- and two-component solutions via adsorption on N-doped activated carbon. Materials, 14(22). https://doi.org/10.3390/ma14227045

Khodapanah, N., Ahamad, I. S., & Idris, A. (2013). Potential of using bio-coagulants indigenous to Malaysia for surface water clarification. Research Journal of Chemistry and Environment, 17(9), 70–75. https://www.researchgate.net/publication/261597552_Potential_of_using_bio-coagulants_indigenous_to_Malaysia_for_surface_water_clarification

Kokalj, A. (2022). Corrosion inhibitors: physisorbed or chemisorbed? Corrosion Science, 196.

https://doi.org/10.1016/j.corsci.2021.109939

Kokalj, A. (2026). Estimating standard adsorption Gibbs energy from corrosion inhibition efficiencies: A case of multilayer adsorption. Corrosion Science, 258. https://doi.org/10.1016/j.corsci.2025.113323

Li, S., & Zhu, J. (2024). One-step oil bath preparation of cobalt-doped MnO2/coconut activated carbon composite with superior zinc ion storage performance. Journal of Energy Storage, 100. https://doi.org/10.1016/j.est.2024.113676

Liang, Cao, S., Liu, C., Zeb, S., Cui, Y., & Sun, G. (2020). Heavy metal adsorption using structurally preorganized adsorbent. RSC Advances, 10(12), 7259–7264. https://doi.org/10.1039/d0ra00125b

Lo, S. F., Wang, S. Y., Tsai, M. J., & Lin, L. D. (2012). Adsorption capacity and removal efficiency of heavy metal ions by Moso and Ma bamboo activated carbons. Chemical Engineering Research and Design, 90(9), 1397–1406. https://doi.org/10.1016/j.cherd.2011.11.020

Mahdavi, M., Ebrahimi, A., Mahvi, A. H., Fatehizadeh, A., Karakani, F., & Azarpira, H. (2018). Experimental data for aluminum removal from aqueous solution by raw and iron-modified granular activated carbon. Data in Brief, 17, 731–738. https://doi.org/10.1016/j.dib.2018.01.063

Melliti, A., Yılmaz, M., Sillanpää, M., Hamrouni, B., & Vurm, R. (2023). Low-cost date palm fiber activated carbon for effective and fast heavy metal adsorption from water: Characterization, equilibrium, and kinetics studies. Colloids and Surfaces A: Physicochemical and Engineering Aspects, 672. https://doi.org/10.1016/j.colsurfa.2023.131775

Mkilima, T., Zharkenov, Y., Abduova, A., Sarypbekova, N., Kudaibergenov, N., Sakanov, K., Zhukenova, G., Omarov, Z., Sultanbekova, P., & Kenzhaliyeva, G. (2024). Utilization of banana peel-derived activated carbon for the removal of heavy metals from industrial wastewater. Case Studies in Chemical and Environmental Engineering, 10. https://doi.org/10.1016/j.cscee.2024.100791

Moujoud, Z., Harrati, A., Manni, A., Naim, A., El Bouari, A., & Tanane, O. (2023). Study of fired clay bricks with coconut shell waste as a renewable pore-forming agent: Technological, mechanical, and thermal properties. Journal of Building Engineering, 68. https://doi.org/10.1016/j.jobe.2023.106107

Muttakin, M., Mitra, S., Thu, K., Ito, K., & Saha, B. B. (2018). Theoretical framework to evaluate minimum desorption temperature for IUPAC classified adsorption isotherms. International Journal of Heat and Mass Transfer, 122, 795–805. https://doi.org/10.1016/j.ijheatmasstransfer.2018.01.107

Mutugi, A., Guzzo, E. C., Koech, M., Koech, M., & Tang, J. (2025). A case report of a 79-year-old female with aluminum toxicity presenting with altered mental status in Eldoret, Kenya. Toxicology Reports, 15. https://doi.org/10.1016/j.toxrep.2025.102128

Othmani, B., Rasteiro, M. G., & Khadhraoui, M. (2020). Toward green technology: a review on some efficient model plant-based coagulants/flocculants for freshwater and wastewater remediation. In Clean Technologies and Environmental Policy (Vol. 22, Issue 5, pp. 1025–1040). Springer Science and Business Media Deutschland GmbH. https://doi.org/10.1007/s10098-020-01858-3

Pandey, A., Kalamdhad, A., & Chandra Sharma, Y. (2023). Recent advances of nanocellulose as biobased adsorbent for heavy metal ions removal: A sustainable approach integrating with waste management. In Environmental Nanotechnology, Monitoring and Management (Vol. 20). Elsevier B.V. https://doi.org/10.1016/j.enmm.2023.100791

Pérez, S., Ulloa, M., Flórez, E., Acelas, N., Ocampo-Pérez, R., Padilla-Ortega, E., & Forgionny, A. (2023). Valorization of lemon peels wastes into a potential adsorbent for simultaneous removal of copper ion (Cu2+) and Congo red from wastewater. Environmental Nanotechnology, Monitoring and Management, 20. https://doi.org/10.1016/j.enmm.2023.100795

Phal, S., Guigui, C., Didi, A., Tan, R., & Bessiere, Y. (2025). Role of natural organic matter on diclofenac adsorption on activated carbon produced from banana peels. Journal of Water Process Engineering, 77. https://doi.org/10.1016/j.jwpe.2025.108495

Ranatunga, K. S., del Rey Castillo, E., & Toma, C. L. (2023). Evaluation of the optimal concrete mix design with coconut shell ash as a partial cement replacement. Construction and Building Materials, 401. https://doi.org/10.1016/j.conbuildmat.2023.132978

Raychaudhuri, S., Raychaudhuri, M., Mohanty, R. K., & Rautaray, S. K. (2025). Effect of treated wastewater on heavy metal accumulation, fish growth and associated implications on consumer health. Journal of the Taiwan Institute of Chemical Engineers, 166. https://

doi.org/10.1016/j.jtice.2024.105652

Ren, Y. S., Ilyas, M., Yasir, M., & Rahman, S. U. (2023). Adsorption of aluminum from aqueous solutions utilizing waste polyethylene terephthalate derived activated carbon. Desalination and Water Treatment, 310, 123–132. https://doi.org/10.5004/dwt.2023.29933

Rouquerol, J., Avnir, D., Fairbridge, C. W., Everett, D. H., Haynes, J. H., Pernicone, N., Ramsay, J. D. F., Sing, K. S. W., & Unger, K. K. (1994). Recommendations for the Characterization of Porous Solids. Pure and Applied Chemistry, 66(8), 1739–1758. https://list.iupac.org/publications/pac/1994/pdf/6608x1739.pdf

Sahmoune, M. N. (2019). Evaluation of thermodynamic parameters for adsorption of heavy metals by green adsorbents. In Environmental Chemistry Letters (Vol. 17, Issue 2, pp. 697–704). Springer. https://doi.org/10.1007/s10311-018-00819-z

Shi, J., Wu, X., Zhao, X., Zhou, J., Liu, S., Li, B., Zhang, J., Li, W., Zeng, X., Wang, X., Wang, S., & Jia, Y. (2024). Remediation of heavy metal-contaminated estuarine sediments by strengthening microbial in-situ mineralization. Applied Geochemistry, 169. https://doi.org/10.1016/j.apgeochem.2024.106051

Song, X., Zhou, X., & Lv, X. (2023). Quantitative evaluation of pore connectivity of shales with a type H3 sorption hysteresis loop. Journal of Asian Earth Sciences, 247. https://doi.org/10.1016/j.jseaes.2023.105595

Tangsathitkulchai, M., Tangsathitkulchai, C., Wongsooksin, K., & Chuyingsakuntip, S. (2012). Removal of residual aluminium-dye complex and aluminium ion from spent natural-dye solution using activated carbons. Engineering Journal, 16(5), 29–43. https://doi.org/10.4186/ej.2012.16.5.29

Waheed, A., Baig, N., Ullah, N., & Falath, W. (2021). Removal of hazardous dyes, toxic metal ions and organic pollutants from wastewater by using porous hyper-cross-linked polymeric materials: A review of recent advances. In Journal of Environmental Management (Vol. 287). Academic Press. https://doi.org/10.1016/j.jenvman.2021.112360

World Health Organization. (2021). A global overview of national regulations and standards for drinking-water quality Second edition. https://iris.who.int/bitstream/handle/10665/350981/9789240023642-eng.pdf?sequence=1#:~:text=The%20GDWQ%20are%20an%20international%20reference%20point%20for,assist%20them%20in%20the%20development%20of%20national%20standards.

Xu, L., Wang, F., Liu, Y., Wang, M., Chen, X., Wang, E., & Yan, J. (2024). Beneficial elements silicon and calcium can be used as supplements to improve the yield and quality of the Mentha spicata L. essential oils. Industrial Crops and Products, 214. https://doi.org/10.1016/j.indcrop.2024.118506

Xu, Y., Jin, Z., Gou, L. F., Bouchez, J., Jin, C., Li, C., Liu-Lu, B., & Deng, L. (2023). Cation exchange controls riverine magnesium isotopes in extremely-high-erosion catchments. Geochimica et Cosmochimica Acta, 363, 1–14. https://doi.org/10.1016/j.gca.2023.10.033

Xu, Y., Jin, Z., Gou, L. F., Galy, A., Jin, C., Chen, C., Li, C., & Deng, L. (2022). Carbonate weathering dominates magnesium isotopes in large rivers: Clues from the Yangtze River. Chemical Geology, 588. https://doi.org/10.1016/j.chemgeo.2021.120677

Zhao, B., Christodoulatos, C., Shi, Q., Ji, M., Sheets, S., & Meng, X. (2026). Effective removal of sulfate and heavy metals from wastewater by ettringite precipitation using aluminum-based sludge. Separation and Purification Technology, 382. https://doi.org/10.1016/j.seppur.2025.135776